

Transformer-based RGB-T Tracking with Channel and Spatial Feature Fusion

Yunfeng Li, Bo Wang*, Ye Li, Zhiwen Yu, Liang Wang

Abstract—Complementary RGB and TIR modalities enable RGB-T tracking to achieve competitive performance in challenging scenarios. Therefore, how to better fuse cross-modal features is the core issue of RGB-T tracking. Some previous methods either insufficiently fuse RGB and TIR features, or depend on intermediaries containing information from both modalities to achieve cross-modal information interaction. The former does not fully exploit the potential of using only RGB and TIR information of the template or search region for channel and spatial feature fusion, and the latter lacks direct interaction between the template and search area, which limits the model’s ability to fully exploit the original semantic information of both modalities. To alleviate these limitations, we explore how to improve the performance of a visual Transformer by using direct fusion of cross-modal channels and spatial features, and propose CSTNet. CSTNet uses ViT as a backbone and inserts cross-modal channel feature fusion modules (CFM) and cross-modal spatial feature fusion modules (SFM) for direct interaction between RGB and TIR features. The CFM performs parallel joint channel enhancement and joint multilevel spatial feature modeling of RGB and TIR features and sums the features, and then globally integrates the sum feature with the original features. The SFM uses cross-attention to model the spatial relationship of cross-modal features and then introduces a convolutional feedforward network for joint spatial and channel integration of multimodal features. Comprehensive experiments show that CSTNet achieves state-of-the-art performance on three public RGB-T tracking benchmarks. Code is available at <https://github.com/LiYunfengLYF/CSTNet>.

Index Terms—RGB-T tracking, Channel Feature Fusion, Spatial Feature Fusion, Transformer Network.

I. INTRODUCTION

RGB-T tracking combines the advantages of the visual modality, which contains more information, and the infrared modality, which is less affected by the environment, to achieve stable tracking of the target in low light and adverse weather conditions. Due to its advantage in processing visual and infrared image sequences, it has a wide range of potential applications in traffic monitoring [3], robot perception [4] and autonomous driving [5].

As a multimodal vision task, how to achieve effective cross-modal interaction plays a crucial role in RGB-T tracking. In previous works, MDNet-based trackers propose a large number of cross-modal feature fusion methods, such as channel feature fusion [6], adapter [7], challenge-aware model [8], spatial-temporal feature fusion [9], multi-scale feature fusion [10], etc. These methods greatly advance the development of RGB-T tracking. However, the MDNet architecture itself makes it difficult for these trackers to extract discriminative deep

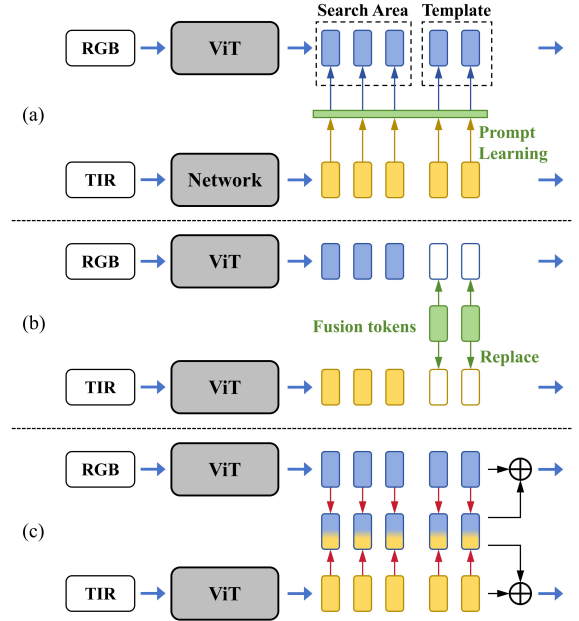


Fig. 1. Comparison between our cross-modal feature fusion method with other Transformer-based RGB-T trackers. (a) TIR features are fused into RGB features by extracting prompts, such as ViPT [1] (b) RGB and TIR features interact through the intermediate tokens, such as TBSI [2] (c) Our approach achieves cross-modal interaction through channel and spatial feature fusion of RGB and TIR features.

feature. Then Siamese-based trackers [11][12][13] further explore the channel fusion methods of cross-modal deep features. However, their sample candidate boxes (RoIs) lack a global receptive field, as only local multimodal features of the search area are used for fusion. Overall, these MDNet-based and Siamese-based methods are limited by their own architecture and do not fully explore the potential of channel and spatial feature fusion. With the introduction of Transformer in RGB-T tracking, some methods use visual prompt learning [1][14] or adapter [15] to achieve better modeling of RGB feature guided by TIR feature, as illustrated in Figure 1 (a), while others are similar to the above methods, as illustrated in Figure 1 (b), like using feature bridging fusion [2], spatial-temporal feature fusion [16], etc. to achieve effective modeling of cross-modal features. Although these methods effectively achieve cross-modal feature interaction based on transformers, they are implemented by extracting intermediate prompt features or using partially fused cross-modal tokens. Their indirect feature interaction leads to a lack of use of the original semantics of multimodal features.

* Corresponding author. Email: cv_heu@163.com.

Based on the above analysis, although cross-modal channel feature fusion has been introduced in some MDNet-based and Siamese-based trackers, the multimodal features they extract limit the performance of the fusion module. For Transformer-based methods, although the multimodal features become better, channel and spatial feature fusion based on direct feature interaction does not receive sufficient attention.

As a basic feature fusion method, channel and feature fusion has significant advantages in the pixel-level interaction between RGB and TIR features. It directly models the original semantics of RGB and TIR features, thus avoiding the loss of key features caused by the use of intermediate tokens. For other RGB-T visual tasks, such as RGB-T semantic segmentation and RGB-T saliency detection, many cross-modal channel and spatial feature fusion modules have been proposed for Transformer-based methods, such as using multimodal channel attention to supplement key information between two modalities and using cross-attention to model spatial representations across-modalities [17], using feature concatenation, channel attention, and multi-level feature fusion module to recursively fuse intermediate features from different stages [18], etc. The success of the above feature fusion module demonstrates the enormous potential for direct interaction between RGB and TIR features in Transformer.

Therefore, this paper aims to combine channel and feature fusion with Visual Transformer (ViT). Specifically, we investigate how to achieve direct interaction of multimodal features in ViT and improve the performance of our tracking pipeline by using the original semantic information from the cross-modal features. Most transformer-based methods design an independent feature fusion module to preserve the powerful feature extraction and relationship modeling capabilities of the ViT. Following this design, the critical problem becomes how to design a channel feature fusion module and a spatial feature fusion module.

In this work, we propose an RGB-T tracker referred to as CSTNet. CSTNet explores the advantages of directly integrating RGB and TIR features in space and channels in ViT. Similar to [2], we design a cross-modal channel feature fusion module (CFM) and a spatial feature fusion (SFM) module, respectively. We cascade them into a block, and insert the blocks into the ViT, which is our backbone. The CFM performs joint channel enhancement and multi-level spatial modeling of multimodal features, and then globally integrates the original semantic and fused semantic information across modal features. The SFM achieves cross-modal feature interaction through cross-attention, and then combines spatial and channel features through convolutional feedforward layers.

Ours main contributions are summarized as follow:

(1) We propose a cross-modal channel feature fusion module (CFM) that first concatenates and linearly fuses RGB and TIR features, then performs channel enhancement and multi-level spatial feature modeling in parallel and sums the output features, and finally globally integrates the hybrid features with the original features.

(2) We propose a cross-modal spatial feature fusion module (SFM) that first aggregates local spatial feature, then models the spatial relationships of multimodal features using cross-

attention module, and finally integrates the spatial and channel information of multimodal features through a convolutional feedforward network.

(3) We propose an RGB-T tracker CSTNet. CSTNet combines channel and spatial feature fusion with Transformer, and achieves effective cross-modal interaction by directly fusing the RGB and TIR features. Comprehensive experiments have shown that our method achieves state-of-the-art performance.

II. RELATED WORK

A. RGB-T Tracking

Some RGB-T trackers propose channel fusion and spatial fusion methods for cross-modal features. For example, DAFNet [6] proposes a channel-attention-based recursive fusion chain to achieve cross-modal and multi-level feature fusion in MDNet. SiamCDA [11] proposes a complementarity aware feature fusion module. It concatenates RGB and TIR features, and then enhances cross-modal features through a joint channel attention module. Finally, it achieves feature fusion through cross-modal residual connection and feature concatenation. SiamTDR [12] concatenates RGB and TIR features and then calculates the weight of channel attention by dynamic convolution to obtain fused feature. The fusion module of SiamMALL [13] is similar to the above methods, except that it replaces the feature concatenation of the last layer with feature addition. MACFT [19] proposes a cross-attention fusion module and a mix-attention fusion module for spatial feature fusion in Transformer. It only performs cross-attention operations on the multimodal features output by its backbone to obtain fused features.

Compared with these channel feature fusion modules, our method not only uses channel enhancement, but also introduces multi-level local spatial feature modeling and global integration module to achieve cross-modal feature fusion. Compared to the spatial fusion module proposed by MACFT [19], our method explores the potential of cross-attention and integrates the spatial representation of the fused feature by convolutional feedforward network. In addition, we insert our modules into different layers of the backbone to achieve cross-modal feature interactions at different stages.

In addition, there are many other effective cross-modal feature fusion methods in RGB-T tracking. BAT [15] proposes a universal bi-directional adapter to achieve interaction between RGB and TIR features in transformer blocks. TBSI [2] uses the fused template as a bridge to achieve information interaction between RGB and TIR modalities in the search area based on the attention mechanism. CAT++ [20] proposes five different attribute-based branches to perceive different challenges, and then fuses the features of different branches through an aggregation interaction module to achieve multimodal tracking. TATrack [16] introduces an online template to model temporal information, and achieves cross-modal feature interaction between the initial template and the online template.

However, these methods achieve cross-modal feature fusion by using intermediate features, prior knowledge, and temporal information. They do not explore the effectiveness of direct

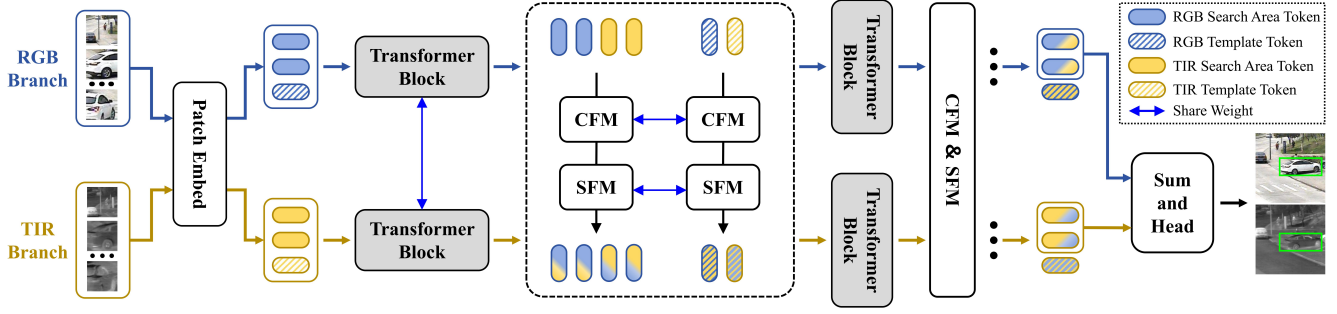


Fig. 2. The overall framework of CSTNet. Our backbone is a bilateral ViT with shared weights. The RGB and TIR image patches are first embedded into tokens and fed into 12 Transformer Blocks. The proposed CFM and SFM perform cross-modal feature fusion on template features and search area features in the network, respectively. They are inserted into 4-th, 7-th, and 10-th layers of the backbone. Finally, the RGB and TIR features of the search area are added, and the prediction head is used to predict the current state of the target.

interaction between RGB and TIR features, which results in the model not being able to benefit from the original semantic interaction between RGB and TIR features. In contrast, our method explores the potential for direct channel and spatial fusion of cross-modal features in the transformer network.

B. Feature fusion for other RGB-T visual tasks

The channel and spatial feature fusion module has been widely applied to other non-sequential RGB-T tasks. CMX [17] uses cross-modal channel and spatial attention to complement and correct multimodal features. It also proposes a feature fusion module based on a cross-attention module and a convolutional feedforward layer for spatial modeling and joint integration of cross-modal features. MMSFormer [18] proposes a multimodal features fusion module based on multi-level feature fusion and channel enhancement. It fuses multimodal features from different stages in the backbone to obtain a robust mixed-modality feature representation of the target. SwinNet [21] performs spatial alignment based on spatial attention on cross-modal features, and then channel attention modules are used to recalibrate RGB and TIR features separately.

Compared to these methods, our method uses the fused feature to help model the association between the template and the search area, rather than using the fused feature to distinguish the category of pixels or to predict the target's boxes. As a result, our modules differ significantly in terms of insertion layers and model design.

III. METHOD

The overall framework of CSTNet is shown in Figure 2. We first embed the template images and search area images into tokens, and then fed the tokens into transformer blocks. Our proposed channel feature fusion module (CFM) and spatial feature fusion module (SFM) are inserted between transformer blocks for cross-modal feature interaction. Finally, the RGB and TIR features of the search area output from the last transformer block are added and fed into the prediction head to obtain the target state. Due to the same processing of template and search area in CFM and SFM, we only show the processing of multimodal features in the search area in sections III-B and III-C.

A. Backbone

We follow the recent RGB-T trackers [2][16] to select ViT [22] as our backbone. The inputs of the backbone are the RGB and TIR template images represented as $z_r, z_t \in R^{H_z \times W_z \times 3}$ and the RGB and TIR search area images are represented as $x_r, x_t \in R^{H_x \times W_x \times 3}$. These four images are first embedded as tokens and positional embeds are added as follows:

$$\begin{aligned} Z_r &= \text{PE}(z_r) + E_z, Z_t = \text{PE}(z_t) + E_z \\ X_r &= \text{PE}(x_r) + E_x, X_t = \text{PE}(x_t) + E_x \end{aligned} \quad (1)$$

where PE denotes Patch Embed function as same in [22]. $Z_r, Z_t \in R^{N_z \times C}$ denote the init feature of RGB and TIR template tokens. $N_z = H_z W_z / p^2$, where p is the down-sampling stride of patch embedding. C is the channel number. $X_r, X_t \in R^{N_x \times C}$ denote the init feature of RGB and TIR search area tokens, where $N_x = H_x W_x / p^2$. E_z and E_x are the positional embeds with the same shape as Z_r and X_r , respectively.

Since the feature extraction and modeling is the same for both modalities, we only discuss the process in the RGB modality. The RGB tokens are concatenated as $H_r = [X_r; Z_r] \in R^{(N_x + N_z) \times C}$, then fed H_r into a series of Transformer [22] blocks.

The proposed cross-modal feature fusion method is represented as $Z_{rt} = f(Z_r, Z_t), X_{rt} = f(x_r, x_t)$ where Z_{rt} denotes the fusion feature of the template and X_{rt} denotes the fusion feature of the search area. After the fusion, the relationship modeling is represented as:

$$\begin{aligned} A &= \text{Softmax}\left(\frac{QK^T}{\sqrt{C}}\right) = \text{Softmax}\left(\frac{[X_{qrt}; Z_{qrt}][X_{krt}; Z_{krt}]^T}{\sqrt{C}}\right) \\ &= \text{Softmax}\left(\frac{[X_{qrt}X_{krt}^T, X_{qrt}Z_{krt}^T; Z_{qrt}X_{krt}^T, Z_{qrt}Z_{krt}^T]}{\sqrt{C}}\right) \end{aligned} \quad (2)$$

where Q, K, V denotes query, key and values matrices, respectively.

From the above formulation, after the fusion, the template features and the search area features used for relationship modeling contain both RGB and TIR semantic information. The multi-level fusion of RGB and TIR features and the joint modeling of cross-modal features improve the model's utilization of multi-level cross-modal semantic information.

B. Channel feature fusion module

Our proposed CFM module aims to integrate RGB and TIR features of templates or search areas into the channel. As shown in Figure 3, CFM contains a channel enhancement module for jointly enhancing key information within channels, a local spatial aggregation module (LSA) for jointly modeling multi-level spatial feature representation, and a global integration module (GIM) for integrating original and fused features.

We first linearly fuse multimodal features, specifically, we concatenate the RGB and TIR features of the search area, and then use a linear layer to obtain the fused feature:

$$X_c = \text{Linear}([X_r; X_t]) \in R^{N_x \times C} \quad (3)$$

where Linear represents the linear layer.

Then, an squeeze-and-excitation (SE) module [23] is used as a channel enhancement unit to achieve channel enhancement of X_c .

$$X_c^{\text{se}} = \text{SE}(X_c) \quad (4)$$

The local spatial aggregation module (LSA) is used to extract multi-level local spatial features and model key representations of mixed multi-level features through a nonlinear layer. Specifically, a linear transformation is first performed on the feature X_c and obtain $X_c^{\text{fc}} = \text{Linear}(X_c) \in R^{N_x \times C}$.

Then we use convolutional blocks to extract multi-level spatial features, represented as:

$$X_c^{\text{msf}} = \text{Conv}_{1 \times 1}(X_c^{\text{fc}}) + \sum_{k \in \{3,5,7\}} \text{DWConv}_{k \times k}(X_c^{\text{fc}}) \quad (5)$$

where Conv and DWConv represent convolutional layer with batch-normalize (BN) and depth-wise separable convolutional layer with BN, respectively.

Another linear layer is used to perform a linear transformation on the fused features, integrating multi-level features and improving its consistency, represented as $X_c^{\text{lsa}} = \text{Linear}(\text{Gelu}(\text{Conv}_{1 \times 1}(X_c^{\text{msf}}))) \in R^{N_x \times C}$, where Gelu represents GELU activate function [24].

After parallel SE and LSA modules, the features are added, represented as $X_c^{\text{add}} = X_c^{\text{se}} + X_c^{\text{lsa}} \in R^{N_x \times C}$. In addition, residual connections are introduced to supplement the original semantic information lost in multimodal features, represented as $X_r^{\text{res}} = X_r + X_c^{\text{add}}$ and $X_t^{\text{res}} = X_t + X_c^{\text{add}}$.

The global integration module (GIM) concatenates RGB and TIR features, and fed it into a multi-layer perceptron (MLP) with residual connection. Then, split the concatenated feature to obtain integrated RGB and TIR features. The process is described as:

$$X_r^{\text{cfm}}, X_t^{\text{cfm}} = \text{Split}([X_r^{\text{res}}; X_t^{\text{res}}] + \text{MLP}([X_r^{\text{res}}; X_t^{\text{res}}])) \quad (6)$$

where Split maps the feature from $R^{N_x \times 2C}$ to two $R^{N_x \times C}$ features. MLP is consist of two linear layers. The X_r^{cfm} and X_t^{cfm} are the CFM output features.

Due to the difference between the template and the search area, GIM is not shared when processing the features between the template and the search area.

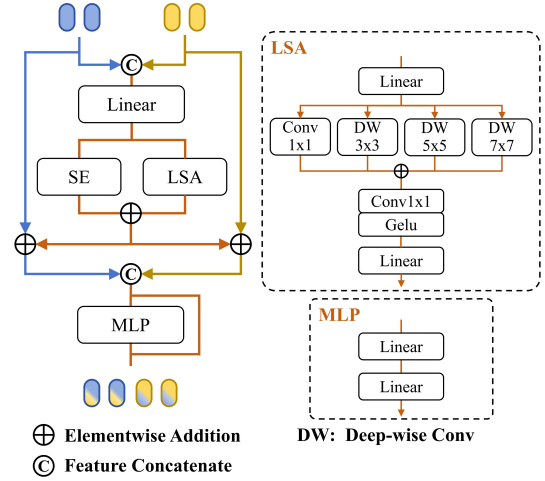


Fig. 3. Illustration of our proposed CFM module. It encompasses a channel enhancement module, which is a SE module [23], a local spatial aggregation module (LSA), and a global integration module (GIM).

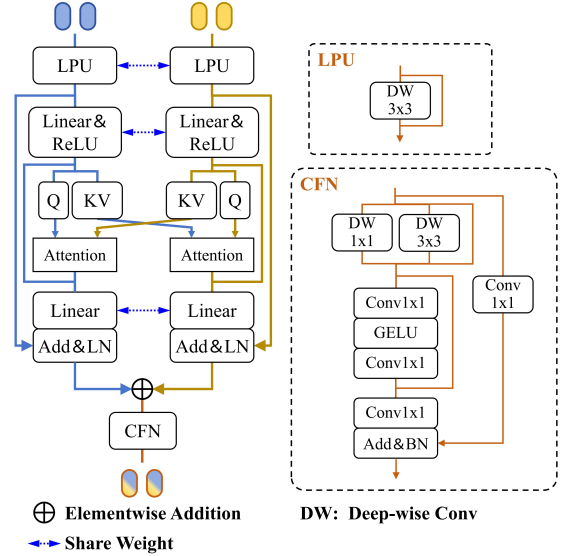


Fig. 4. Illustration of our proposed SFM module. It encompasses a local perception unit (LPU), a cross-attention module and a convolutional feedforward network (CFN).

C. Spatial feature fusion module

Our proposed SFM module aims to model spatial relationships in cross-modal features and to integrate the channel and spatial features of the RGB and TIR modalities through a convolutional feedforward network. As shown in Figure 4, the SFM contains a local perception unit (LPU), a cross-attention module and a convolutional feedforward network (CFN).

We first use a local perception unit (LPU) to aggregate local spatial information, represented as:

$$\begin{aligned} X_r^{\text{lpu}} &= X_r^{\text{cfm}} + \text{DWConv}_{3 \times 3}(X_r^{\text{cfm}}) \\ X_t^{\text{lpu}} &= X_t^{\text{cfm}} + \text{DWConv}_{3 \times 3}(X_t^{\text{cfm}}) \end{aligned} \quad (7)$$

Then a cross-attention module is used to achieve spatial modeling of cross-modal features. Specifically, a non-linear full-connection layer is used and represented as $X_r^{\text{res}}, X_r^{\text{attn}} =$

Split(ReLu(Linear^s(X_r^{lpu}))), where Linear^s is a linear layer shared by RGB and TIR branches. After that, a linear layer is used to obtain Query: X_r^q = Linear(X_r^{attn}), another linear layer is used to obtain Key: X_r^k and Value: X_r^v, represented as X_r^k, X_r^v = Split(Linear(X_s^{attn})). The TIR X_t^q, X_t^k, X_t^v are obtained through the same way.

The cross-attention process of RGB and TIR features is described as follows:

$$\begin{aligned} X_r^{cross} &= \text{Attention}(Q : X_r^q, K : X_t^k, V : X_t^v) \\ X_t^{cross} &= \text{Attention}(Q : X_t^q, K : X_r^k, V : X_r^v) \end{aligned} \quad (8)$$

Then we use residual connections and a shared linear layer to adjust the features and add them up, the process is described as:

$$\begin{aligned} X_r^{add} &= \text{LN}_r(X_r^{cfm} + \text{Linear}^s(X_r^{cross} + X_r^{res})) \\ X_t^{add} &= \text{LN}_t(X_t^{cfm} + \text{Linear}^s(X_t^{cross} + X_t^{res})) \end{aligned} \quad (9)$$

where LN_r and LN_t are different layer-normalize layers.

Then, we add the features X_r^{add} and X_t^{add} to achieve feature point-level interaction between the multimodal features.

$$X_{rt}^{add} = X_r^{add} + X_t^{add} \quad (10)$$

Due to the differences between RGB and TIR features, the directly added feature requires further spatial and channel integration. Therefore, a convolutional feedforward network (CFN) is introduced. In the CFN, we first perform spatial integration on the fused feature. The process can be written as follows:

$$X_{rt}^{local} = X_{rt}^{add} + \sum_{k \in \{1,3\}} \text{DWConv}_{k \times k}(X_{rt}^{add}) \quad (11)$$

Then, we nonlinearly integrate the channel feature of the fused feature, represented as:

$$X_{rt}^{act} = X_{rt}^{local} + \text{Conv}_{1 \times 1}^{\text{down}}(\text{Gelu}(\text{Conv}_{1 \times 1}^{\text{up}}(X_{rt}^{local}))) \quad (12)$$

where Conv_{1×1}^{up} maps the feature from R^C to R^{2×C} and Conv_{1×1}^{down} maps the feature from R^{2×C} to R^C.

In addition, we use a 1x1 convolutional block and a skip connection with a 1x1 convolutional block to adjust the features, the process is described as:

$$X_{rt}^{adj} = \text{BN}(\text{Conv}_{1 \times 1}^{\text{adj}}(X_{rt}^{act}) + \text{Conv}_{1 \times 1}^{\text{res}}(X_{rt}^{act})) \quad (13)$$

where Conv_{1×1}^{adj} and Conv_{1×1}^{res} both map the feature from R^C to R^C.

Finally, we add X_{rt}^{sfm} to the original RGB feature X_r and the original TIR feature X_t to obtain the fused features as:

$$X_r^{\text{sfm}} = X_{rt}^{\text{adj}} + X_r, \quad X_t^{\text{sfm}} = X_{rt}^{\text{adj}} + X_t \quad (14)$$

where X_r^{sfm} and X_t^{sfm} are the output features of SFM.

D. Head and Loss

The RGB and TIR features of the search area output by the last Transformer block are represented as X_r^{output} and X_t^{output}. We add them up to obtain the mixed feature, described as:

$$X_{rt}^{\text{output}} = X_r^{\text{output}} + X_t^{\text{output}} \quad (15)$$

where X_{rt}^{output} is the input of our prediction head.

Following the design of [22] and [2], we adopt a fully convolutional center-head [25] to predict the state of the target.

We use the weight focal loss [26] to train the classification branch and the l1 loss and the wise-IoU loss [27] to train the box regression branch. The total training loss of CSTNet is:

$$L_{total} = L_{cls} + \lambda_{iou} L_{iou} + \lambda_{l1} L_1 \quad (16)$$

where λ_{iou} = 2 and λ_{l1} = 5 are hyper-parameters as same in [2].

IV. EXPERIMENTS

A. Datasets and Evaluation Metrics

LasHeR [28] is a large-scale dataset benchmark that contains 1224 sequences with 730K frame pairs. It is divided into 19 challenging attributes, which are No Occlusion (NO), Partial Occlusion (PO), Total Occlusion (TO), Hyaline Occlusion (HO), Out-of-View (OV), Low Illumination (LI), High Illumination (HI), Abrupt Illumination Variation (AIV), Low Resolution (LR), Deformation (DEF), Background Clutter (BC), Similar Appearance (SA), Thermal Crossover (TC), Motion Blur (MB), Camera Moving (CM), Frame Lost (FM), Fast Motion (FM), Scale Variation (SV), Aspect Ratio Change (ARC). RGBT234 [29] is a classic benchmark for RGB-T tracking that contains 234 sequences. RGBT234 [29] has 12 challenging attributes, they are no occlusion (NO), partial occlusion (PO), heavy occlusion (HO), low illumination (LI), low resolution (LR), thermal crossover (TC), deformation (DEF), fast motion (FM), scale variation (SV), motion blur (MB), camera moving (CM) and background clutter (BC). RGBT210 [30] is another classic RGB-T tracking benchmark that contains 210 sequences.

Following the metrics used by current most RGB-T trackers, precision rate (PR) and success rate (SR) are employed to evaluate different trackers on RGBT210 [30] and RGBT234 [29], and precision rate (PR), normalized precision rate (NPR) and success rate (SR) are employed to evaluate the trackers on LasHeR [28].

B. Implementation Details

CSTNet is implemented based on Ubuntu 20.04, using Python 3.9 and Pytorch 1.13.0. It is trained on a platform with two NVIDIA RTX A6000 GPUs over 20 epochs, which took roughly 6 hours. LasHeR [28] training set is used for training our model. In each epoch, we sample 60k image pairs, with a total batch-size of 64. The total learning rate is set to 2e⁻⁵ for the backbone and 2e⁻⁶ for feature fusion modules. It is decayed by 10× after 15 epochs. We use AdamW as the optimizer with 1e⁻⁴ weight decay. The size of template and search area is set to 128×128 and 256×256, respectively. Our CFM and SFM modules are cascaded and inserted into the 4-th, 7-th, and 10-th layers of the ViT. We use the ViT model weight of the RGB-T tracker [2] as the pre-training weight. CSTNet achieves speed at 62 FPS on GPU GTX 3090Ti.

TABLE I
COMPARISON WITH STATE-OF-THE-ART TRACKERS ON RGBT210, RGBT234 AND LAsHeR [28] TESTING SET. HIGHER VALUE INDICATE BETTER PERFORMANCE. THE BEST TWO RESULTS ARE SHOWN IN RED AND BLUE FONTS.

Method	Source	Baseline	RGBT210 [30]		RGBT234 [29]		LasHeR [28]		
			PR	SR	PR	SR	PR	NPR	SR
TFNet [31]	TCSVT2021	MDNet	77.7	52.9	80.6	56.0	-	-	-
DMCNet [32]	TNNLS22	MDNet	79.7	55.9	83.9	59.3	49.0	43.1	35.5
APFNet [8]	AAAI2022	MDNet	79.9	54.9	82.7	57.9	50.0	43.9	36.2
X-Net [33]	Arxiv2023	MDNet	-	-	85.2	62.2	50.8	-	44.6
CAT++ [20]	TIP2024	MDNet	82.2	56.1	84.0	59.2	50.9	44.4	35.6
SiamCDA [11]	TCSVT2021	Siamese	-	-	76.0	56.9	-	-	-
DFAT [34]	Inf Fusion23	Siamese	-	-	75.8	55.2	-	-	-
SiamMLAA [13]	TMM2023	Siamese	-	-	78.6	58.4	-	-	-
MFNet [35]	IVC2022	DCF	-	-	84.4	60.1	59.7	55.4	46.7
LSAR [36]	TCSVT2023	DCF	-	-	78.4	55.9	-	-	-
CMD [37]	CVPR2023	DCF	-	-	82.4	58.4	59.0	54.6	46.4
AMNet [38]	TCSVT2024	DCF	-	-	85.5	60.7	61.4	55.9	47.7
ProTrack [14]	ACM MM2022	Transformer	79.5	59.9	78.6	58.7	53.8	-	42.0
ViPT [1]	CVPR2023	Transformer	83.5	61.7	83.5	61.7	65.1	-	52.5
MACFT [19]	Sensors2023	Transformer	-	-	85.7	62.2	65.3	-	52.5
RSFNet [39]	ISPL2023	Transformer	-	-	86.3	62.2	65.9	-	52.6
DFMTNet [40]	IEEE Sens.J23	Transformer	-	-	86.2	63.6	65.1	-	52.0
TBSI [2]	CVPR2023	Transformer	85.3	62.5	87.1	63.7	69.2	65.7	55.6
STMT [41]	Arxiv2024	Transformer	83.0	59.5	86.5	63.8	67.4	63.4	53.7
TATrack [16]	Arxiv2024	Transformer	85.3	61.8	87.2	64.4	70.2	66.7	56.1
BAT [15]	AAAI2024	Transformer	-	-	86.8	64.1	70.2	-	56.3
TransAM [38]	TCSVT2024	Transformer	-	-	87.7	65.5	70.2	66.0	55.9
CSTNet	-	Transformer	86.0	63.5	88.4	65.2	71.5	67.9	57.2

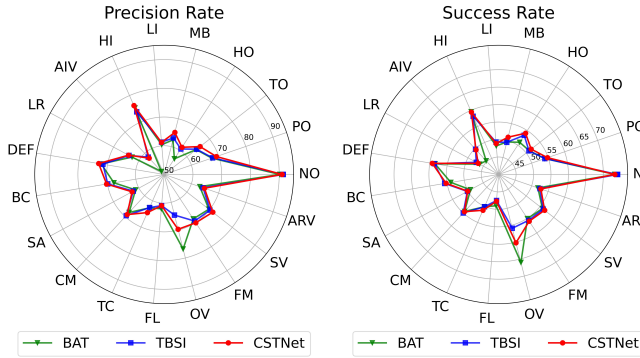


Fig. 5. The SR and PR scores of CSTNet, TBSI [2] and BAT [15] under different attributes on LasHeR [28].

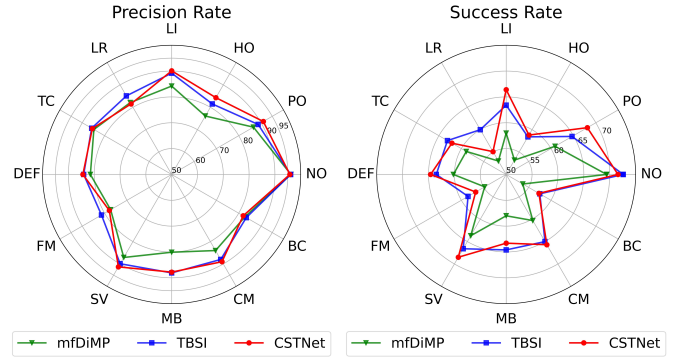


Fig. 6. The SR and PR scores of CSTNet, TBSI [2], mfdiMP [42], under different attributes on RGBT234 [29].

C. Comparison with State-of-the-art Methods

1) *Comparison methods:* To evaluate the effectiveness of our method, we compared it with RGB-T trackers from recent years, including 5 MDNet-based trackers, including TFNet [31], DMCNet [32], APFNet [8], X-Net [33], CAT++ [20], 3 Siamese-based trackers, including SiamCDA [11], SiamMALL [13], DFAT [34], 4 DCF-based trackers MFNet [35], LSAR [36], CMD [37], AMNet [38] and 11 transformer-based trackers, including ProTrack [14], ViPT [1], MACFT [19], RSFNet [39], DFMTNet [40], TBSI [2], STMT [41], BAT [15], TATrack [16], TransAM [38].

2) *Evaluation on LasHeR Dataset:* The trackers are evaluated on LasHeR [28] and the results are reported on Table

I. CSTNet achieves state-of-the-art performance. Compare to other Transformer-based trackers, CSTNet outperforms TATrack [16] and TransAM [38] by both 1.3% in PR, 1.2% and 1.9% in NPR, 1.1% and 1.3% in SR, respectively. In addition, the PR and SR of CSTNet are 1.3% and 0.9% higher than BAT [15]. In addition, CSTNet surpasses all other MDNet-based and Siamese-based methods. The results show that CSTNet achieves better cross-modal feature interaction and better performance.

In addition, we evaluate CSTNet, TBSI [2] and BAT [15] on 19 attributes of LasHeR [28] dataset. As shown in Figure 5, CSTNet outperforms other transformer-based trackers in many attributions. Compared to TBSI [2], CSTNet achieves more

TABLE II

ABLATION STUDIES OF OUR PROPOSED CFM AND SFM MODULES IN THE TRACKING PIPELINE.

Method	PR	NPR	SR
RGBT	70.0	66.3	56.0
RGBT+CFM	70.5 (+0.5)	67.0 (+0.7)	56.5 (+0.5)
RGBT+CFM&SFM	71.5 (+1.5)	67.9 (+1.6)	57.2 (+1.2)

TABLE III

ABLATION OF THE DIFFERENT METHODS FOR FUSING SEARCH AREA CROSS-MODAL FEATURES.

Method	PR	NPR	SR
concat	70.0	66.4	55.1
add	71.5	67.9	57.2

competitive performance in challenges such as occlusion (HO, PO and SO), thermal crossover (TC), out-of-view (OV) and motion blur (MB). Compare to BAT [15], CSTNet has better performance in attributes such as heavy occlusion (HO), abrupt illumination variation (AIV), and background clutter (BC). However, the PR and SR of CSTNet on ARV, FL, SA, AIV and LI attributes are insufficient, which proves that CSTNet needs to further improve the robustness and feature discrimination of the model.

3) *Evaluation on RGBT234 Dataset*: The trackers are evaluated on RGBT234 [29] and the results are reported on Table I. Compared to the TransAM [38], CSTNet improves the PR by 0.7%. Compared to the BAT [15], CSTNet improves the PR and SR by 1.6% and 1.1%, respectively. The results show that CSTNet sets a new state-of-the-art benchmark.

We further evaluate our proposed CSTNet, TBSI [2], and mfDiMP [42] on 12 attributes of RGBT234 [29] dataset. As shown in Figure 6, CSTNet achieves better performance on most attributes compared to other trackers. However, it has insufficient success rate in heavy occlusion (HO) and low resolution (LR) background clutter (BC) and fast motion (FM). This indicates that it has shortcomings in dealing with the challenges such as missing key features and interference from background features.

4) *Evaluation on RGBT210 Dataset*: The trackers are evaluated on RGBT210 and the results are reported on Table I. CSTNet outperforms all other RGB-T trackers. The PR, SR of CSTNet are 0.7%, 1.0% higher than TBSI [2]. In addition, CSTNet achieves an SR score of 63.5%, outperforms STMT [41] and TATrack [16] by 4.0% and 1.7%, respectively. The experimental results demonstrate that CSTNet outperforms all other trackers and achieves state-of-the-art performance.

D. Ablation Studies

To investigate the individual influence of different components, we conduct ablation studies on CSTNet and report the results for PR, NPR and SR on LasHeR [28].

1) *Component Analysis*: We first evaluate the effect of summing RGB and TIR features and the CFM and SFM modules on the performance of the tracker. *RGBT* denotes adding the RGB and TIR features of the search area output by the

TABLE IV

ABLATION OF THE DIFFERENT COMPONENTS OF CFM.

CFM			PR	NPR	SR
SE	LSA	GIM			
			69.5	65.8	55.8
✓			70.5	66.8	56.3
✓	✓		70.8	67.1	56.7
✓	✓	✓	71.5	67.9	57.2

TABLE V

ABLATION OF THE DIFFERENT COMPONENTS OF SFM.

SFM			PR	NPR	SR
LPU	Cross-Attn	CFN			
			70.5	67.0	56.5
✓			70.6	67.1	56.5
✓	✓		71.0	67.4	56.8
✓	✓	✓	71.5	67.9	57.2

shared ViT backbone, and then predicting the target state. The pretrain-model of the baseline is [2]. The impact of different pre-trained models on the tracker will be discussed in Section IV-D4. As shown in Table II, an improvement of 0.5% and 1.0% in term of PR, 0.7% and 0.9% in term of NPR and 0.5% and 0.7% in term of SR is obtained by the contribution of the CFM module and the SFM module, respectively. In addition, they achieved a total of 1.5%, 1.6%, and 1.2% improvement in term of PR, NPR and SR, respectively. Overall, both our proposed CFM and SFM modules are important.

In addition, we separately investigate the impact of concatenating or adding the RGB and TIR features of the search area output from the backbone on the tracking performance. *concat* is used by TBSI [2], which means that the RGB and TIR features of the search area are concatenated and then a 1x1 convolution is used to reduce the dimension. As shown in Table III, the addition of RGB and TIR features in the search area achieves better performance. Our method avoids the feature representation bottleneck caused by the 1x1 convolution dimension reduction, allowing the model to benefit from the direct addition of RGB and TIR features in the search area.

2) *Ablation of CFM*: We evaluate the contributions of the each component of the CFM. As shown in Table IV, When the CFM module is removed from the model, the PR and SR are 69.5% and 55.8%, respectively. Adding the SE module improves the PR by 1.0% and the SR by 0.5%. Then, using the LSA module achieves better performance, with increases of 0.3% for SR and 0.4% for PR, respectively. Next, using the GIM module to integrate global features results in an improvement of 0.7% for PR and 0.5% for SR, respectively. Overall, all three modules in CFM contribute to improving the performance of our model.

3) *Ablation of SFM*: The contribution of each component to the SFM is measured. Table V shows the results. The contribution of the LPU is an improvement of 0.1% for PR. The Cross-attention module improves the PR by 0.4% and SR by 0.3%, respectively. The CFN module improves the PR by 0.5% and SR by 0.4%. Overall, all three components of the

TABLE VI
ABLATION STUDIES OF DIFFERENT PRE-TRAINED MODELS.

Pre-train Model	P	NP	SR
-	55.6	51.7	42.2
ImageNet [43]	59.1	56.0	47.3
SOT [22]	69.7	65.9	55.8
RGBT [2]	71.5	67.9	57.2

TABLE VII
ABLATION STUDIES OF DIFFERENT INSERT LAYERS OF OUR CFM AND SFM MODULES.

Layers			P	NP	SR
4	7	10			
			70.0	66.3	56.0
✓			70.4	66.6	56.3
✓	✓		70.9	67.1	56.8
✓	✓	✓	71.5	67.9	57.2

SFM are effective.

4) *Ablation of pre-trained models*: We explore the impact of different pre-trained models on our proposed CSTNet in terms of performance. CSTNet without pretraining and CSTNet with ImageNet pretraining are unable to converge in 20 epochs, therefore we increase their learning rate by 10x. The results are shown in Table VI, CSTNet with RGB-T pretraining achieves the best performance. It outperforms CSTNet with SOT pretraining by 1.8% for PR and 1.4% for SR. This shows that using the RGB-T pre-trained model can further improve the performance of the tracker.

5) *Inserting Layers of CFM and SFM*: In addition, We conduct ablation experiments on different insert layers of our proposed CFM and SFM modules. The results are reported in Table VII. Inserting the CFM and SFM modules in the 4-th layer of ViT improves the PR by 0.4% and the SR by 0.3%. Inserting the modules in the 7th and 10th layers of ViT further improves the performance of the tracker. Overall, inserting our CFM and SFM modules into these three layers effectively achieves feature fusion at different stages and improves model performance.

E. Visualization

1) *Heatmap*: We explore how CSTN utilizes RGB and TIR modalities to improve model performance. As shown in Figure 7, in the bikeboyright sequence which is a typical daytime traffic scenario, our proposed CSTNet effectively uses RGB and TIR modalities to better predict the target state. In the biketurnright sequence which is a typical nighttime scenario, although CSTNet is interfered with in RGB feature, the model still makes a correct prediction in fused features under the reference of TIR feature. In the whitebikebelow and yellowgirl118 sequences, CSTNet improves target state prediction in high illumination and partial occlusion challenges by complementing the features of RGB and TIR modalities. CSTNet effectively achieves cross-modal feature interaction.

In addition, we compare the cross-modal feature interaction performance of CSTNet and other Transformer-based methods (TBSI [2] and BAT [15]) in four typical sequences of the

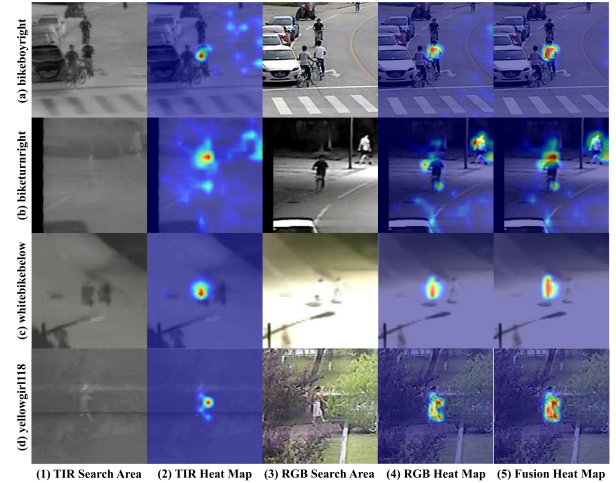


Fig. 7. Visualization of heat maps of RGB feature, TIR feature and fusion feature of the search area on LasHeR [28] based on Grad-CAM. The *Fusion Heat Map* represents the heatmap of the sum feature of the RGB and TIR modalities. The fusion feature’s heat map is only displayed in RGB modality. (a) bikeboyright (frame 301), (b) biketurnright (frame 46), (c) whitebikebelow (frame 165), (d) yellowgirl118 (frame 65).

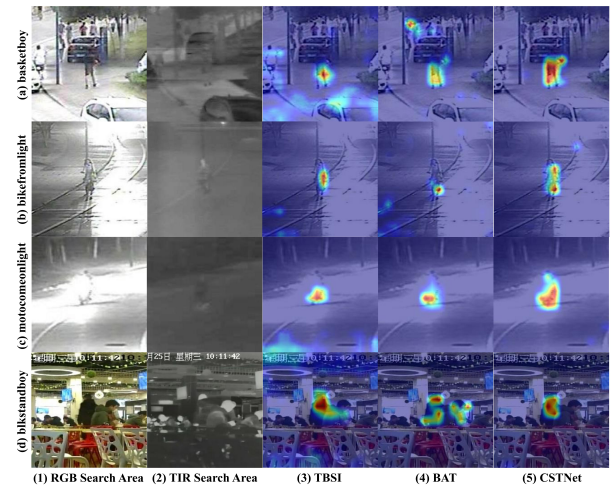


Fig. 8. Visualization of heat maps of the fusion feature of CSTNet, TBSI [2] and BAT [15] on LasHeR [28] based on Grad-CAM. The fusion feature’s heat map is only displayed in RGB modality. (a) basketboy (frame 48), (b) bikefromlight (frame 138), (c) motocomeonlight (frame 31), (d) blkstandboy (frame 128).

LasHeR [28] dataset, as shown in Figure 8. Our proposed CSTNet achieves direct interaction between RGB and TIR original semantics through channel and spatial fusion of multimodal features. In the basketboy, bikefromlight, and motocomeonlight sequences, CSTNet achieves richer utilization of cross-modal appearance features. In the blkstandboy sequence, CSTNet has better discrimination for similar appearance. Overall, CSTNet demonstrates the benefits of direct cross-modal feature interaction on model performance.

2) *Tracking Results*: We select four representative sequences from the Lasher dataset to show some of the results of CSTNet and other previous state-of-the-art RGB-T trackers. As shown in Figure 9, in the rightdarksingleman sequence,

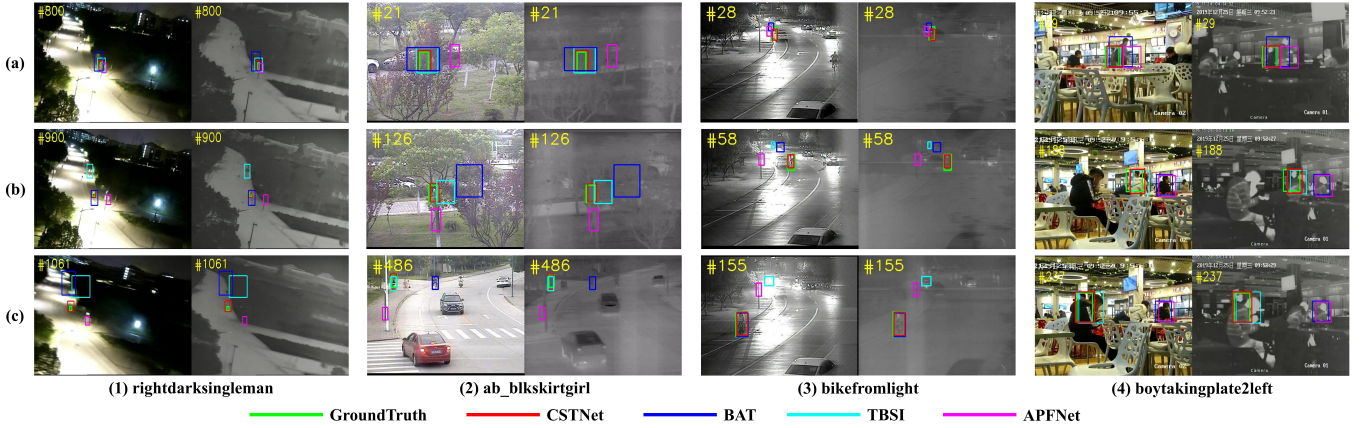


Fig. 9. Visualized comparisons of CSTNet with TBSI [2], BAT [15] and APFNet [8] on four sequences from LasHeR [28] dataset.

when other trackers briefly lose the target due to low light and camera shake, our proposed CSTNet still tracks the target stably, demonstrating the better robustness of CSTNet. In the ab_blkskirtgirl sequence, when the target is frequently occluded, other trackers usually lose the target briefly, while our CSTNet does not lose the target. In the bikefromlight sequence, when the scene is highly illuminated, our CSTNet accurately distinguishes the target from surrounding clutter, resulting in better performance. In the boytakingplate2left sequence, our CSTNet better integrates the RGB and TIR features of the target, resulting in better performance in partial occlusion and similar appearance challenges. Overall, our proposed CSTNet has stronger discriminative ability and better tracking performance.

V. CONCLUSION

In this paper, we present a new RGB-T tracker CSTNet. CSTNet explores the advantages of using channel and spatial feature fusion to achieve direct interaction between RGB and TIR features. CSTNet contains two novel cross-modal feature interaction modules, CFM and SFM. The CFM achieves joint channel enhancement of RGB and TIR features, joint multi-level modeling, and global integration of fused features and original features. The SFM achieves spatial mutual modeling of RGB and TIR features and joint spatial and channel integration of multimodal features. Comprehensive experiments show that the direct interaction between RGB and TIR features improves the performance of the model, and our proposed CSTNet achieves state-of-the-art performance on three challenging RGB-T tracking benchmarks.

VI. ACKNOWLEDGMENTS

This research is funded by the National Key Research and Development Program of China, grant number 2023YFC2809104, by the National Natural Science Foundation of China, grant number 52371350, and by the National Key Laboratory Foundation of Autonomous Marine Vehicle Technology, grant number 2024-HYHXQ-WDZC03.

REFERENCES

- [1] J. Zhu, S. Lai, X. Chen, D. Wang, and H. Lu, "Visual prompt multi-modal tracking," in *Proceedings of the IEEE/CVF conference on computer vision and pattern recognition*, 2023, pp. 9516–9526.
- [2] T. Hui, Z. Xun, F. Peng, J. Huang, X. Wei, X. Wei, J. Dai, J. Han, and S. Liu, "Bridging search region interaction with template for rgb-t tracking," in *Proceedings of the IEEE/CVF Conference on Computer Vision and Pattern Recognition*, 2023, pp. 13 630–13 639.
- [3] T. Alldieck, C. H. Bahnsen, and T. B. Moeslund, "Context-aware fusion of rgb and thermal imagery for traffic monitoring," *Sensors*, vol. 16, no. 11, p. 1947, 2016.
- [4] L. Chen, L. Sun, T. Yang, L. Fan, K. Huang, and Z. Xuanyuan, "Rgb-t slam: A flexible slam framework by combining appearance and thermal information," in *2017 IEEE International Conference on Robotics and Automation (ICRA)*. IEEE, 2017, pp. 5682–5687.
- [5] I. Shopovska, L. Jovanov, and W. Philips, "Deep visible and thermal image fusion for enhanced pedestrian visibility," *Sensors*, vol. 19, no. 17, p. 3727, 2019.
- [6] Y. Gao, C. Li, Y. Zhu, J. Tang, T. He, and F. Wang, "Deep adaptive fusion network for high performance rgbt tracking," in *Proceedings of the IEEE/CVF International conference on computer vision workshops*, 2019, pp. 0–0.
- [7] C. Long Li, A. Lu, A. Hua Zheng, Z. Tu, and J. Tang, "Multi-adapter rgbt tracking," in *Proceedings of the IEEE/CVF international conference on computer vision workshops*, 2019, pp. 0–0.
- [8] Y. Xiao, M. Yang, C. Li, L. Liu, and J. Tang, "Attribute-based progressive fusion network for rgbt tracking," in *Proceedings of the AAAI Conference on Artificial Intelligence*, vol. 36, no. 3, 2022, pp. 2831–2838.
- [9] C. Wang, C. Xu, Z. Cui, L. Zhou, T. Zhang, X. Zhang, and J. Yang, "Cross-modal pattern-propagation for rgb-t tracking," in *Proceedings of the IEEE/CVF Conference on computer vision and pattern recognition*, 2020, pp. 7064–7073.
- [10] Q. Xu, Y. Mei, J. Liu, and C. Li, "Multimodal cross-layer bilinear pooling for rgbt tracking," *IEEE Transactions on Multimedia*, vol. 24, pp. 567–580, 2021.
- [11] T. Zhang, X. Liu, Q. Zhang, and J. Han, "Siamcda: Complementarity- and distractor-aware rgb-t tracking based on siamese network," *IEEE Transactions on Circuits and Systems for Video Technology*, vol. 32, no. 3, pp. 1403–1417, 2021.
- [12] G. Wang, Q. Jiang, X. Jin, Y. Lin, Y. Wang, and W. Zhou, "Siamtdr: Time-efficient rgbt tracking via disentangled representations," *IEEE Transactions on Industrial Cyber-Physical Systems*, 2023.
- [13] M. Feng and J. Su, "Learning multi-layer attention aggregation siamese network for robust rgbt tracking," *IEEE Transactions on Multimedia*, 2023.
- [14] J. Yang, Z. Li, F. Zheng, A. Leonardis, and J. Song, "Prompting for multi-modal tracking," in *Proceedings of the 30th ACM international conference on multimedia*, 2022, pp. 3492–3500.
- [15] B. Cao, J. Guo, P. Zhu, and Q. Hu, "Bi-directional adapter for multi-modal tracking," in *Proceedings of the AAAI Conference on Artificial Intelligence*, vol. 38, no. 2, 2024, pp. 927–935.

- [16] H. Wang, X. Liu, Y. Li, M. Sun, D. Yuan, and J. Liu, "Temporal adaptive rgbt tracking with modality prompt," *arXiv preprint arXiv:2401.01244*, 2024.
- [17] J. Zhang, H. Liu, K. Yang, X. Hu, R. Liu, and R. Stiefelwagen, "Cmx: Cross-modal fusion for rgb-x semantic segmentation with transformers," *IEEE Transactions on Intelligent Transportation Systems*, 2023.
- [18] M. K. Reza, A. Prater-Bennette, and M. S. Asif, "Multimodal transformer for material segmentation," *arXiv preprint arXiv:2309.04001*, 2023.
- [19] Y. Luo, X. Guo, M. Dong, and J. Yu, "Learning modality complementary features with mixed attention mechanism for rgb-t tracking," *Sensors*, vol. 23, no. 14, p. 6609, 2023.
- [20] L. Liu, C. Li, Y. Xiao, R. Ruan, and M. Fan, "Rgt tracking via challenge-based appearance disentanglement and interaction," *IEEE Transactions on Image Processing*, vol. 33, pp. 1753–1767, 2024. [Online]. Available: <https://api.semanticscholar.org/CorpusID:268252011>
- [21] Z. Liu, Y. Tan, Q. He, and Y. Xiao, "Swinnet: Swin transformer drives edge-aware rgb-d and rgb-t salient object detection," *IEEE Transactions on Circuits and Systems for Video Technology*, vol. 32, no. 7, pp. 4486–4497, 2021.
- [22] B. Ye, H. Chang, B. Ma, S. Shan, and X. Chen, "Joint feature learning and relation modeling for tracking: A one-stream framework," in *European conference on computer vision*. Springer, 2022, pp. 341–357.
- [23] J. Hu, L. Shen, and G. Sun, "Squeeze-and-excitation networks," in *Proceedings of the IEEE conference on computer vision and pattern recognition*, 2018, pp. 7132–7141.
- [24] D. Hendrycks and K. Gimpel, "Gaussian error linear units (gelus)," *arXiv preprint arXiv:1606.08415*, 2016.
- [25] K. Duan, S. Bai, L. Xie, H. Qi, Q. Huang, and Q. Tian, "Centernet: Keypoint triplets for object detection," in *2019 IEEE/CVF International Conference on Computer Vision (ICCV)*, 2019, pp. 6568–6577.
- [26] H. Law and J. Deng, "Cocornet: Detecting objects as paired keypoints," in *Proceedings of the European conference on computer vision (ECCV)*, 2018, pp. 734–750.
- [27] Z. Tong, Y. Chen, Z. Xu, and R. Yu, "Wise-iou: Bounding box regression loss with dynamic focusing mechanism," *arXiv preprint arXiv:2301.10051*, 2023.
- [28] C. Li, W. Xue, Y. Jia, Z. Qu, B. Luo, J. Tang, and D. Sun, "Lasher: A large-scale high-diversity benchmark for rgbt tracking," *IEEE Transactions on Image Processing*, vol. 31, pp. 392–404, 2021.
- [29] C. Li, X. Liang, Y. Lu, N. Zhao, and J. Tang, "Rgb-t object tracking: Benchmark and baseline," *Pattern Recognition*, vol. 96, p. 106977, 2019.
- [30] C. Li, N. Zhao, Y. Lu, C. Zhu, and J. Tang, "Weighted sparse representation regularized graph learning for rgb-t object tracking," in *Proceedings of the 25th ACM international conference on Multimedia*, 2017, pp. 1856–1864.
- [31] Y. Zhu, C. Li, J. Tang, B. Luo, and L. Wang, "Rgt tracking by trident fusion network," *IEEE Transactions on Circuits and Systems for Video Technology*, vol. 32, no. 2, pp. 579–592, 2022.
- [32] A. Lu, C. Qian, C. Li, J. Tang, and L. Wang, "Duality-gated mutual condition network for rgbt tracking," *IEEE Transactions on Neural Networks and Learning Systems*, pp. 1–14, 2022.
- [33] Z. Ding, H. Li, R. Hou, Y. Liu, S. Xie, D. Zhou, and J. Cao, "X modality assisting rgbt object tracking," *arXiv preprint arXiv:2312.17273*, 2023.
- [34] Z. Tang, T. Xu, H. Li, X.-J. Wu, X. Zhu, and J. Kittler, "Exploring fusion strategies for accurate rgbt visual object tracking," *Information Fusion*, vol. 99, p. 101881, 2023.
- [35] Q. Zhang, X. Liu, and T. Zhang, "Rgb-t tracking by modality difference reduction and feature re-selection," *Image and Vision Computing*, vol. 127, p. 104547, 2022. [Online]. Available: <https://www.sciencedirect.com/science/article/pii/S0262885622001767>
- [36] J. Liu, Z. Luo, and X. Xiong, "Online learning samples and adaptive recovery for robust rgb-t tracking," *IEEE Transactions on Circuits and Systems for Video Technology*, 2023.
- [37] T. Zhang, H. Guo, Q. Jiao, Q. Zhang, and J. Han, "Efficient rgb-t tracking via cross-modality distillation," in *Proceedings of the IEEE/CVF Conference on Computer Vision and Pattern Recognition (CVPR)*, June 2023, pp. 5404–5413.
- [38] T. Zhang, X. He, Q. Jiao, Q. Zhang, and J. Han, "Amnet: Learning to align multi-modality for rgb-t tracking," *IEEE Transactions on Circuits and Systems for Video Technology*, 2024.
- [39] Z. Yu, H. Fan, Q. Wang, Z. Li, and Y. Tang, "Region selective fusion network for robust rgb-t tracking," *IEEE Signal Processing Letters*, 2023.
- [40] M. Li, P. Zhang, M. Yan, H. Chen, and C. Wu, "Dynamic feature-memory transformer network for rgbt tracking," *IEEE Sensors Journal*, 2023.
- [41] D. Sun, Y. Pan, A. Lu, C. Li, and B. Luo, "Transformer rgbt tracking with spatio-temporal multimodal tokens," *arXiv preprint arXiv:2401.01674*, 2024.
- [42] L. Zhang, M. Danelljan, A. Gonzalez-Garcia, J. Van De Weijer, and F. Shahbaz Khan, "Multi-modal fusion for end-to-end rgb-t tracking," in *Proceedings of the IEEE/CVF International conference on computer vision workshops*, 2019, pp. 0–0.
- [43] K. He, X. Chen, S. Xie, Y. Li, P. Dollár, and R. Girshick, "Masked autoencoders are scalable vision learners," in *Proceedings of the IEEE/CVF conference on computer vision and pattern recognition*, 2022, pp. 16 000–16 009.